PERGAMON

Scripta mater. 43 (2000) 1033–1038

Scripta MATERIALIA

www.elsevier.com/locate/scriptamat

TENSILE CREEP PROPERTIES OF δ-Bi_2O_3

Jeffrey L. Grabowski and David C. Dunand
Department of Materials Science and Engineering, Northwestern University, Evanston, IL 60208, USA

(Received April 18, 2000)
(Accepted in revised form July 11, 2000)

Keywords: Functional ceramics; Binary oxides; Creep; Phase transformations

Introduction

Bi_2O_3 is an excellent ceramic candidate for transformation-mismatch plasticity because of its low melting point, its allotropic nature and the rapid creep rate of its high-temperature δ-phase. Transformation-mismatch plasticity, which has been reported in many polymorphic metals, alloys and composites [1], is a deformation mechanism taking place during a phase transformation: internal mismatch stresses produced by the coexistence of the two polymorphic phases are biased by a small externally-applied tensile stress, thus producing a strain increment. Such compressive strain increments were indeed measured by Johnson *et al.* [2] for Bi_2O_3 subject to a single thermal excursion about the allotropic transformation under a compressive stress. For metals and alloys subjected to repeated allotropic cycling under a tensile stress, these strain increments can be accumulated up to total tensile strains well in excess of 100%, a phenomenon known as transformation superplasticity [1]. We describe in another publication [3] such tensile transformation superplasticity experiments for Bi_2O_3, for which a good understanding of tensile isothermal creep properties under small stresses is however first necessary. With all prior creep studies of Bi_2O_3 having been conducted in compression and at relatively high stresses [4,5], the purpose of the present paper is to investigate the low-stress creep behavior δ-Bi_2O_3 in tension. Also, we investigate whether thermal cycling about the allotropic transformation under stress affects the subsequent isothermal creep properties.

Experimental Procedures

Electronic-grade, 99.9995% pure, α-Bi_2O_3 powders (from Metal Specialties Products, Fairfield, CT) were sieved to -45 μm, and the fine fraction was ground with 6 wt. % de-ionized water for 5 min. before being dry-pressed at 65 MPa for 90 s into rectangular bars. After evaporating the water, the bars were cold isostatically pressed at 275 MPa for 10 min. The bars were then heated on an alumina substrate to 700°C at a rate of 5°C/min and sintered for 24 hr. in air to approximate dimensions of $57 \times 17 \times 8$ mm. The density of each as-sintered bar was measured according to ASTM C-373 and found to be between 97.6–100% for all specimens used in mechanical tests (except for specimen S3 with a relative density of 95.7%). These densities were much higher than the value of 86 ± 2% reported by Vilette and Kampe [4] after cold-pressing at 560 MPa and sintering at 700°C for 24 h, and similar to those achieved by Zaripov *et al.* [5] (>98%) after hot-pressing at 650°C and 500 MPa.

After polishing to 0.3 μm alumina, a sintered specimen with 98% relative density was thermally etched in the α-phase for 1 hr. in air at the sintering temperature of 700°C. The mean grain diameter

PII: S1359-6462(00)00531-5

of as-sintered α-Bi_2O_3 was 13 μm, somewhat larger than the 9 μm value reported in Ref. [4,5]. The sintered bars were machined into flat tensile specimens with overall dimensions of 50.1 × 16.7 × 2.5 mm and with a gage section 16.7 mm long and 4.6 mm wide. The radius at the end of the gage was small (less than 1 mm). Every surface was hand-polished with 600 grit SiC paper to remove any small chips incurred during machining and ultrasonically cleaned in acetone prior to testing.

Two types of mechanical tests were used. A first series of tests (denominated S in the following) were conducted on a servo-mechanical MTS machine operated under constant tensile load conditions where the elongation of specimens was determined from cross-head displacement and temperature was measured with a thermocouple at the gauge length. After soaking at the test temperature of 760±5°C for 10 min., the load was applied and a minimum creep rate was measured on each of six specimens (S1-S5, S7) at a constant tensile stress in the range of 0.09–0.78 MPa. Specimens were subsequently cycled about the transformation range under load, as reported in more detail in Refs. [3,6]. One specimen (S6) was subjected to increasing stress values from 0.14 MPa to 0.78 MPa at 760°C to determine the stress exponent n. Subsequently, specimen S6 was tested again at a lower stress of 0.30 MPa, thermally cycled 10 times under that stress, and then crept at 760°C at 0.36 MPa.

A dead-load tensile creep apparatus was used for 8 additional isothermal and cycling specimens which are denominated C in the following. Specimen elongation was measured from load-train travel outside the hot zone and specimen temperature was determined with a thermocouple at the center of the gauge length. Two tests were carried out at a tensile stress of 0.30 MPa and increasing temperatures (710–760°C for specimen C5 and 680–740°C for specimen C6) to determine a creep activation energy. To insure that these specimens were in the δ-phase during the creep tests, they were first heated under minimal load to 760°C then cooled to the lowest temperature of the test while still in the δ-phase. Furthermore, six creep specimens (C1-C4, C7-C8) were tested in air at 760±5°C at one or two tensile stress values in the range of 0.10–0.50 MPa and were subsequently subjected to thermal cycling under load about the allotropic temperature [3,6]. Except for specimens C1 and C4, fracture occurred before post-cycling creep could be measured. The pre- and post-cycling creep rates of specimen C1 were measured after 6 cycles at 0.11 MPa and 10 cycles at 0.21 MPa, both between 595 and 755°C. Post-cycling creep was measured in specimen C4 after 6 cycles at 0.31 MPa between 600 and 760°C.

Results and Discussion

After mechanical loading, a primary creep region was observed where the strain-rate decreased smoothly over a strain of about 0.3–0.8%. Subsequently, a secondary creep regime characterized by a steady-state, minimum creep rate was established over a strain of about 1.5–4%. Figure 1a shows a double logarithmic plot of the minimum strain-rate $\dot{\epsilon}$ at 760°C as a function of the stress σ, according to the power-law creep equation:

$$\dot{\epsilon} = K \cdot \sigma^n \cdot \exp\left(-\frac{Q}{RT}\right) \tag{1}$$

where K is a constant, n the stress exponent, Q the activation energy, R the gas constant and T the absolute temperature. An average stress exponent n = 1.3 is determined from a best-fit line in Fig. 1a, which also shows a band corresponding to a deviation by ±50% from the best-fit line, corresponding to the typical creep experimental error expected at low stresses [7]. According to Eq. (1), Fig. 1b gives the temperature dependence of the minimum strain rate for specimens C5 and C6, from which activation energies of 200 kJ/mol and 130 kJ/mol respectively are calculated, with an average value of 165 kJ/mol. For this average activation energy, the power-law constant determined from data in Fig. 1a has a value of $K = 6.0 \cdot 10^3$ $MPa^{-1.3} \cdot s^{-1}$.

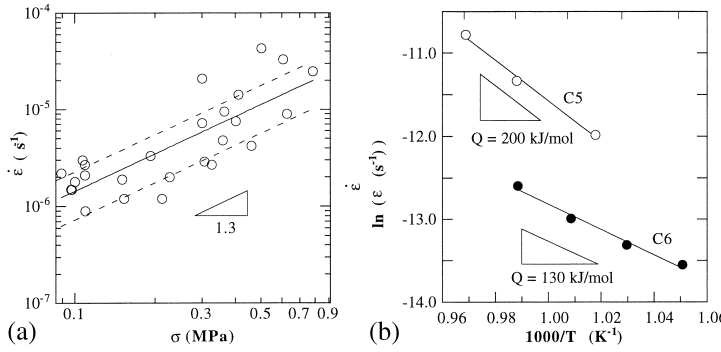

Figure 1. a. Plot of strain rate vs. stress for δ-Bi_2O_3 at 760°C showing an average stress exponent n = 1.3. Dotted band corresponds to a typical creep error of ± 50% from the best-fit solid line. b. Logarithmic plot of strain rate vs. inverse temperature for δ-Bi_2O_3 at 0.3 MPa, yielding activation energies Q = 200 and 130 kJ · mol^{-1} for specimens C5 and C6, respectively.

We are only aware of two studies of the high-temperature creep behavior of Bi_2O_3 under isothermal conditions. First, Zaripov *et al*. [5] measured the compressive flow stress of α-Bi_2O_3 at 650°C under constant strain rates in the range of $6 \cdot 10^{-5}$–$5 \cdot 10^{-3}$ sec^{-1} and for stresses in the range 8–30 MPa. In the low strain-rate region, they measured a stress exponent of about 2.5 and large compressive strains on the order of 75%. Examination of the samples after deformation indicated that the equiaxed grains were stable, the texture was decreased and grain boundary sliding was the dominant deformation mechanism. Based on these features, they identified the deformation mechanism of α-Bi_2O_3 as microstructural superplasticity. In contrast to the above results, Vilette and Kampe [4] found that α-Bi_2O_3 deformed in compression only 1% before cracking at 700°C, which may have been due to the larger amount of porosity of their specimens. However, these authors found that δ-Bi_2O_3 exhibited extensive compressive ductility under constant strain rate conditions. They reported stress exponents and activation energies from creep in the stress range 0.6–2.5 MPa and temperature range of 750–800°C.

Figure 2 shows our tensile creep data plotted together with the compressive creep data of Vilette and Kampe [4]. Our highest stress at 760°C (0.8 MPa) is very close to their lowest stress at 750°C (0.95 MPa), and the discrepancy in strain rate for these two data points is about a factor 4, somewhat larger than the typical scatter in our data. We note that Vilette and Kampe's specimens exhibited high porosity (14%, as compared to our values which are less than 2.4%), so that densification could have contributed

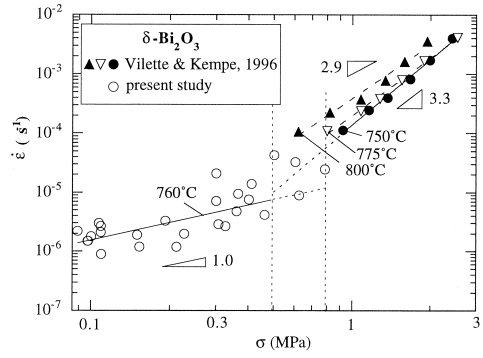

Figure 2. Double logarithmic plot of strain rate vs. stress for δ-Bi_2O_3 at 760°C (from Fig. 1a) and at 750–800 °C (from Vilette and Kampe [4]).

to their measured compressive strain rate. Also, our experiments were conducted under constant load, while they used constant strain-rate conditions and observed some strain-hardening. Nevertheless, Fig. 2 shows that the two sets of data are mutually consistent if a change of stress exponent occurs at about 0.5–0.8 MPa. The stress exponent n = 3.3 for the data of Vilette and Kampe at higher stresses (0.95–2.5MPa) is indicative of dislocation creep, as originally suggested by these authors. Using our data point up to 0.5 MPa (and thus neglecting our four highest stress points in the transition range of 0.5–0.8 MPa), the best-fit slope gives a stress exponent n = 1.0, suggestive of diffusional creep or grain-boundary sliding. For comparison purpose in the following, it is mathematically more convenient (and statistically as accurate) to describe the whole data set (0.1–0.8 MPa) with a single stress exponent n = 1.3, rather than using n = 1.0 for 0.1–0.5 MPa and n = 3.3 for 0.5–0.8 MPa. Together with varying initial porosity and cracking which are discussed later, different initial grain sizes in the δ-phase can contribute to the relatively high sample-to-sample variability observed in our creep data; this is because the diffusional creep regime, unlike the dislocation creep regime, is sensitive to grain size. We note that while the grain size in the δ-phase cannot be observed at room temperature, it can be expected to be comparable to the measured α-phase value of 13 μm, since grain growth is inhibited by pores which dictate the steady-state grain size. However, variations in porosity among specimens may have lead to variations in grain sizes for both α- and δ-phases.

Vilette and Kampe [4] determined activation energies from two sets of experiments at 775°C and 800°C over a stress range from 0.5 MPa to 3.0 MPa, and reported values decreasing with stress from about 250 to about 210 kJ/mol. Given their small temperature range of 25 K, these values are in reasonable agreement with our specimen C5 (Q = 200 kJ/mol, Fig. 1b), measured over 50 K for a stress of 0.3 MPa. There is however a significant discrepancy with specimen C6 (Q = 130 kJ/mol, Fig. 1b), which also shows a strain rate lower by a factor of about 4 as compared to specimen C5 at the same nominal stress of 0.3 MPa. Again, it is possible that the differences in both activation energies and strain rates between specimens C5 and C6 in Fig. 1b may be due to variations in δ-Bi_2O_3 grain sizes, leading to different contributions from the two deformation mechanisms. Cracking may also have occurred in specimen C5 because of higher porosity levels and contributed to the measured strain rate, as discussed in more detail later. Creep is expected to be controlled by the self-diffusion of Bi^{3+}, because oxygen anions have a much higher mobility than bismuth cations in δ-Bi_2O_3. An Arrhenius plot of bismuth self-diffusion coefficient (measured by Palkar *et al.* [8] at 700°C, 750°C and 780°C on pressed and sintered pellets of δ-Bi_2O_3) gives an activation energy of 160 kJ/mol in good agreement with our average activation energy for creep.

When characterizing a metallic system for creep at low strain rates, typical experimental error on strain rates is $\pm$50%, which can be subdivided roughly equally between errors in testing parameters (*e.g.*, temperature and stress) and errors due to microstructural differences from specimen to specimen [7]. The latter effect is expected to be more important in ceramics than in metals because of the relatively large residual porosity and high brittleness of ceramics. Higher porosity is expected to lead to higher creep rates both directly (by reducing the load-bearing area of the specimen) and indirectly (by increasing the propensity for cracking and by reducing the grain size). The effect of initial porosity is illustrated in Fig. 3a which shows that the seven samples with a high porosity (arbitrarily chosen as larger than 0.5%) all exhibited creep rates higher than the best fit line. Eliminating from the data set those seven specimens gives a stress exponent n = 1.2 which is only slightly smaller than the value of n = 1.3 calculated taking all data into account. Similarly, the predicted magnitude of the strain rate is decreased only by a small amount (10–30%) in the stress range of interest.

Also shown in Fig. 3a are the six data points (crossed symbols) collected on the same specimen (S6) under conditions of increasing applied stress, except for the second point near 0.3 MPa which was collected last. Ignoring the point at the highest stress where dislocation creep may be active (Fig. 2), these data points show a stress exponent n = 1.4, close to the expected value, and are shifted to the

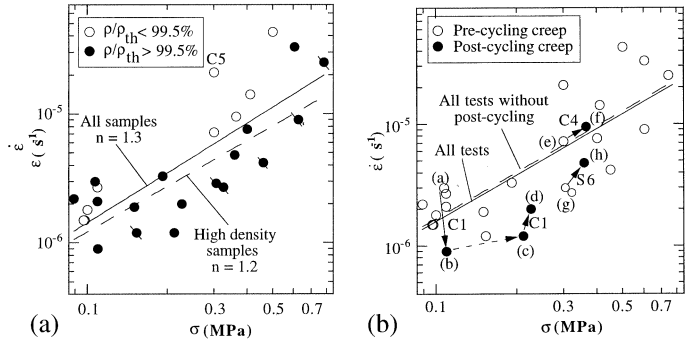

Figure 3. a. Comparison of strain rates for initial specimen relative density above and below 99.5%. Crossed symbols correspond to multiple tests on the same specimen (S6). b. Comparison of strain rates for tests C1, C4 and S6 conducted before and after thermal cycling about the phase transformation of Bi_2O_3.

lower range of creep rate, as expected from the low 0.1% porosity of that specimen. This indicates that once the δ-Bi_2O_3 grain size had been established after the phase transformation, subsequent grain growth or recrystallization (which were suspected to occur in the study of Vilette and Kampe [4]) had no significant effect for the low range of stresses in the present study (specimen S6 was tested for the longest time in the present study). Finally, the higher strain rates previously noted in specimen C5 as compared to specimen C6 (Fig. 1b) also correlate with the different porosities of these two specimens (97.9% and 99.1%, respectively, Fig. 3a). The activation energy determined from the denser specimen C6 (Q = 130 kJ/mol) is thus probably more accurate than that for specimen C5 (Q = 200 kJ/mol).

Figure 3b shows a comparison of creep rates before and after thermal cycling in specimens C1, C4 and S6, which are discussed in detail in the following. For specimen C1, the post-cycling creep rate after 6 thermal cycles at 0.11 MPa (point (b) in Fig. 3b) was three times slower than the pre-cycling rate (point (a)). One explanation may be that a steady-state creep rate had not yet been achieved before cycling (point (a)). Subsequent deformation during thermal cycling at 0.11 MPa allowed the specimen to progress from the primary to the secondary creep regime, leading to a lower post-cycling creep (point (b)). Another explanation is that the δ-Bi_2O_3 grain size was larger after thermal cycling, thus lowering the strain rate. Point (c) shows the strain rate after the stress was increased to 0.21 MPa. After 10 thermal cycles, the stress had increased to 0.23 MPa due to area reduction, and the post-cycling creep rate at point (d) was somewhat higher than expected. While the rate increase from point (c) to point (d) is well within experimental error, cracks observed along the gauge length after cycling may have contributed to the faster deformation. The pre-cycling creep of specimen C4 (point (e)) is close to the best-fit line prediction. After 6 thermal cycles, the stress increased due to reduced cross-section and the strain rate correspondingly increased to point (f), as expected from the best-fit stress exponent. Similarly, for specimen S6, the increase in stress after 10 cycles lead to an increase in strain rate from point (g) to point (h) which was only slightly higher than predicted by the best-fit stress-exponent. For this specimen too, a crack was observed in the gauge length after cycling, leading to fracture shortly after post-cycling creep was achieved.

In summary, while thermal cycling can produce cracking and possibly grain size changes in δ-Bi_2O_3, the four cycling experiments shown in Fig. 3b indicate that there is no significant change, within experimental error, in creep properties as a result of thermal cycling. This is further illustrated by calculating a linear fit in Fig. 3b to all creep data except post-cycling creep: the stress exponent is unchanged at n = 1.3 for all data, and the best-fit line is only slightly shifted to higher strain rates. These observations are in disagreement with Johnson *et al.* [2] who reported that both the α- and δ-phases exhibited large drops in isothermal compressive creep rates after thermal cycling about the phase

transformation. A possible explanation is that densification and/or grain growth occurred in their experiments.

Conclusions

Isothermal tensile creep tests were performed on δ-Bi_2O_3 (with an initial grain size of 13 μm in the α-phase) in the stress range of 0.1–0.8 MPa.

- A stress exponent of n = 1.3 is measured at 760°C in the stress range of 0.1–0.8 MPa or n = 1.0 in the range of 0.1–0.5 MPa. A stress exponent of n = 2.9–3.3 was reported by Vilette and Kampe [4] for compressive creep data at a somewhat higher stress range of 0.6–3 MPa and over a tempe-rature range 750–800°C. Together with our data points in the range 0.5–0.8 MPa, this suggests that δ-Bi_2O_3 transitions from a low-stress deformation regime (diffusional creep and/or grain-boundary sliding) to a high-stress regime (dislocation creep) at a stress of about 0.5–0.8 MPa.
- An average activation energy of Q = 165 kJ/mol is determined from two experiments in the range of 680–760°C for a stress of 0.30 MPa. This value is lower than that reported in the dislocation-creep regime (Q = 210–250 kJ/mol [4]) but similar to the activation energy of self-diffusion for Bi^{3+} (Q = 160 kJ/mol [8]).
- Significant scatter exists in the measured creep rates and may be due to sample-to-sample variation in initial δ-Bi_2O_3 grain sizes (important in diffusional creep) and in the density of cracks and pores (important for tensile tests). Specimens with higher initial porosity were indeed found to deform at higher rates than average.
- Creep rates before and after multiple thermal cycles about the allotropic range under stress were altered only slightly, indicating that microstructural changes due to cycling (cracking, grain growth and recrystallization) are negligible within experimental error.

Acknowledgments

This research was sponsored by the Army Research Office (Contract Number DAAH004-95-1-0629).

References

1. D. C. Dunand, in International Conference on Thermomechanical Processing of Steels and Other Materials, pp. 1821–1830 TMS, Warrendale, PA (1997).
2. C. A. Johnson, R. C. Bradt, and J. H. Hoke, J. Am. Ceram. Soc. 58, 37 (1975).
3. D. C. Dunand, and J. L. Grabowski, J. Am. Ceram. Soc. accepted for publication.
4. A. Vilette and S. L. Kampe, J. Mater. Res. 11, 1433 (1996).
5. N. G. Zaripov, O. A. Kalibyshev, and O. M. Kolnogorov, Phys. Solid State. 35, 1051 (1993).
6. J. L. Grabowski, M.S. Thesis, Northwestern University (1998).
7. M. S. Loveday, in Characterisation of High-Temperature Materials—Mechanical Testing, ed. I. Curbishley, pp. 43–107, Institute of Metals, London (1988).
8. G. D. Palkar, D. N. Sitharamarao, and A. K. Dasgupta, Trans. Farad. Soc. 59, 2634 (1963).